④

OFFICE OF NAVAL RESEARCH

Contract No. N00014-85-K-0129

Work Unit No. 431a007

Technical Report No. 2

# THE MEASUREMENT OF INFRARED SPECTRA OF DENSE CERAMICS BY SPECULAR REFLECTANCE SPECTROSCOPY

by

Mary Bliss, Barbara L. Walden, and William White

Materials Research Laboratory
The Pennsylvania State University
University Park, PA 16802

Prepared for Publication in

The Journal of the American Ceramic Society

*Reproduction in whole or in part is permitted for any purpose of the United States Government.*

*This document has been approved for public release and sale; its distribution is unlimited.*

SECURITY CLASSIFICATION OF THIS PAGE

# REPORT DOCUMENTATION PAGE

1a. REPORT SECURITY CLASSIFICATION
Unclassified

1b. RESTRICTIVE MARKINGS

2a. SECURITY CLASSIFICATION AUTHORITY

2b. DECLASSIFICATION / DOWNGRADING SCHEDULE

3. DISTRIBUTION / AVAILABILITY OF REPORT
Approved for public release, distribution unlimited.

4. PERFORMING ORGANIZATION REPORT NUMBER(S)
No. 2

5. MONITORING ORGANIZATION REPORT NUMBER(S)
N00014-85-K-0129

6a. NAME OF PERFORMING ORGANIZATION
The Pennsylvania State University

6b. OFFICE SYMBOL (If applicable)

6c. ADDRESS (City, State, and ZIP Code)
210 Materials Research Laboratory
University Park, PA 16802

7a. NAME OF MONITORING ORGANIZATION
Office of Naval Research
Dr. Robert Schwartz

7b. ADDRESS (City, State, and ZIP Code)
Code 373
Naval Weapons Center
China Lake, CA 93555-6001

8a. NAME OF FUNDING / SPONSORING ORGANIZATION

8b. OFFICE SYMBOL (If applicable)

9. PROCUREMENT INSTRUMENT IDENTIFICATION NUMBER

8c. ADDRESS (City, State, and ZIP Code)

10. SOURCE OF FUNDING NUMBERS

| PROGRAM ELEMENT NO | PROJECT NO | TASK NO | WORK UNIT NO |
|---|---|---|---|
| | | | |

11. TITLE (Include Security Classification)
The Measurement of Infrared Spectra of Dense Ceramics by Specular Reflectance Spectroscopy

12. PERSONAL AUTHOR(S)
Mary Bliss, Barbara L. Walden, and William B. White

13a. TYPE OF REPORT
Technical

13b. TIME COVERED
FROM ________ TO ________

14. DATE OF REPORT (Year, Month, Day)
July 17, 1989

15. PAGE COUNT
19

16. SUPPLEMENTARY NOTATION

17. COSATI CODES

| FIELD | GROUP | SUB-GROUP |
|---|---|---|
| | | |
| | | |

18. SUBJECT TERMS (Continue on reverse if necessary and identify by block number)

19. ABSTRACT (Continue on reverse if necessary and identify by block number)

It is shown that high quality IR specular reflectance spectra can be obtained from polished surface of dense ceramics. The reflectance spectra can be deconvoluted by the Kramers-Kronig transformation to yield absorption spectra or the real and imaginary parts of the dielectric function. IR line shapes and peak wavenumbers are comparable to single crystal data providing that the particle size is small compared with the IR wavelengths of interest. For non-cubic structures, the spectra are a superposition of polarization components. Modes separated by less than a band width are merged into a single band thus limiting the resolution of the measurement procedure. Grain size effects were modeled using the spectra of single crystal and polycrystal quartz as an example.

20. DISTRIBUTION / AVAILABILITY OF ABSTRACT
☒ UNCLASSIFIED/UNLIMITED ☐ SAME AS RPT ☐ DTIC USERS

21. ABSTRACT SECURITY CLASSIFICATION

22a. NAME OF RESPONSIBLE INDIVIDUAL

22b. TELEPHONE (Include Area Code)

22c. OFFICE SYMBOL

DD FORM 1473, 84 MAR

83 APR edition may be used until exhausted
All other editions are obsolete

SECURITY CLASSIFICATION OF THIS PAGE

# THE MEASUREMENT OF INFRARED SPECTRA OF DENSE CERAMICS BY SPECULAR REFLECTANCE SPECTROSCOPY

Mary Bliss* +, Barbara L. Walden, and William B. White* **
Materials Research Laboratory
The Pennsylvania State University
University Park, PA 16802

## Abstract

It is shown that high quality IR specular reflectance spectra can be obtained from polished surfaces of dense ceramics. The reflectance spectra can be deconvoluted by the Kramers-Kronig transformation to yield absorption spectra or the real and imaginary parts of the dielectric function. IR line shapes and peak wavenumbers are comparable to single crystal data providing that the particle size is small compared with the IR wavelengths of interest. For non-cubic structures, the spectra are a superposition of polarization components. Modes separated by less than a band width are merged into a single band thus limiting the resolution of the measurement procedure. Grain size effects were modeled using the spectra of single crystal and polycrystal quartz as an example.

---

Work supported by the Office of Naval Research

* Member of the American Ceramic Society

\+ Present address: General Electric Co., PO Box 2908, MS 032, Largo, FL 34649.

** Also Affiliated with the Department of Geosciences

## I. Introduction

There are many motivations for wanting to know the infrared spectra of ceramic materials including investigations of fundamental phonon spectra: research on the optical properties of IR-transmitting materials, structure and bonding studies relating to force constants and bond strengths, the identification of aerosol species in the Earth's atmosphere (1), The modeling of radiance spectra of other planets (2), superconductivity investigations (3), and studies of order disorder phenomena, crystallization phenomena, soft modes, and other ferroic properties. Traditionally there have been several approaches to this problem.

One approach is to measure polarized infrared reflectance spectra from oriented single crystals and then to construct absorption spectra or the imaginary part of the dielectric function either by classical oscillator fits or by Kramers-Kronig transforms of the reflectance spectra (4). Another approach is to measure diffuse reflectance spectra, a measurement only possible with the high energy throughput of Fourier transform spectrometers, and to use Kubelka-Munck functions to extract the absorbance spectrum (5). Specular reflectance has also been measured on powder compacts and the reflectance peaks interpreted directly without further deconvolution (6).

The most common approach, unfortunately widely used in the ceramics community, is to borrow a methodology originally developed for organic compounds. Fine grained powders are dispersed in a dielectric medium, typically KBr or polyethylene. Cold-pressed compacts are prepared from the dispersions and the spectra are measured by direct transmission through the compacts. The powder method works fine for organic materials and other covalent compounds but the infrared line shapes become progressively less accurate for materials with a greater degree of polar character. The phonon dynamics of such powders is dominated by the existence of a polarization charge at the surface of each crystallite which gives rise to a series of surface modes whose frequencies lie between those of the longitudinal and transverse modes of the bulk crystal. These vibrations are strongly modified in turn by the powder density and the dielectric constant of the embedding medium (7). The end result, which has been known for more than 20 years (8), is that not only are line shapes dramatically broadened and distorted in the powder spectra of most ceramic materials but the blind assignment of band wavenumbers based on these spectra can result in errors by amounts as great as 50 percent of the true values.

The objective of the present paper is to examine the specular reflectance spectra of some dense polycrystalline ceramic materials and to determine the extent to which one can obtain valid infrared spectra from them. Reflectance measurements have been shown to produce useful spectra on such cubic materials as the thorium phosphide structure $SrLa_2S_4$ (9) and perovskite structure ceramics (10). In this paper we extend the investigation to non-cubic materials where the ceramic consists of an assemblage of randomly distributed optically anisotropic grains. The approach is empirical; ceramic materials are examined for which good single crystal data are available in the literature. A detailed comparison is made between the spectra of single crystal quartz and those of polycrystalline quartz of various grain sizes. It is shown that the polycrystalline spectra can be predicted from the single crystal spectra using simplified assumptions involving the grain size.

## II. Experimental Procedures

The specimens used as test objects were either dense ceramics or natural materials (Table I). Specimens were cut into slabs, polished, and the slabs used directly for measurement. The quartz single crystal was oriented and slabs were cut parallel and perpendicular to the c-crystallographic axis. The slabs were each polished with 1 μm diamond paste, etched for ten minutes with a 10 wt% ammonium bifluoride solution, and then repolished with cerium oxide. The polycrystalline silicas were polished with 1 um alumina and then given a final polish with cerium oxide without etching. The limestone was polished with 1 μm alumina on felt. Both alumina and zinc selenide ceramics were obtained as slabs and measurements were made on the as-received surfaces.

Infrared spectra were measured with a specular reflectance attachment on a Fourier transform infrared spectrometer (a). The micro-specular reflectance sample holder attachment (b) accepts the one cm-diameter beam of the interferometer and focuses it down to 5 mm at the sample. Although not strictly necessary for the present study, additional focusing in the sample compartment allows the use of smaller specimens. Typically 256 interferograms were collected, co-added, and the Fourier transform obtained with the computer on the spectrometer. Data obtained using the KBr beam-splitter (400 - 4000 $cm^{-1}$) were run through the Fourier transform with a phase correction obtained from the reference aluminum mirror. This point is of importance because the usual phase correction in the software produces artifacts in the final spectra (11).

The Fourier transform produced a reflectance spectrum which was then transformed via Kramers Kronig analysis to yield the complex dielectric function (12). The effective resolution with the superimposition of these two mathematical transforms is on the order of 5 wavenumbers for the data spacing (1 -2 wavenumbers) and the number of collected interferograms that were used. The band wavenumbers indicated on the spectra were obtained by measuring the midpoint of the band at half maximum.

In order to have traditional powder spectra for comparison, powder samples of several of the materials were prepared with 1 - 5 mg of powder dispersed in KBr (above 580 wavenumbers) or painted onto a polyethylene plate (below 580 wavenumbers). Transmission spectra were then measured from these powder specimens using the Fourier transform infrared spectrometer.

## III. Infrared Reflectance Spectra of Ceramic Materials

The least complex example is ZnSe with the cubic sphalerite structure which has a single IR-active vibrational mode. Fig. 1 shows the reflectance spectrum of a hot-pressed, optically transparent, infrared window material. The Kramers Kronig analysis yields the imaginary part of the dielectric constant which shows a single sharp band. The band wavenumber of 207 $cm^{-1}$ agrees with the 207 $cm^{-1}$ published value measured on single crystal ZnSe (13). The absorption spectrum obtained by transmission through a pressed powder pellet yields a band which is much broader than the dielectric loss band and has much the same shape as the original reflectance band. However, the powder IR spectrum of this somewhat covalent material is at least an approximation to the bulk vibrational spectrum.

Alumina is a highly polar material with mainly ionic bonding. Infrared absorption is very intense and there is a large separation between transverse and longitudinal optic modes (14). Fig. 2 shows the reflectance spectrum and dielectric loss spectrum for a thin slab of tape-cast, dense, polycrystalline alumina. For comparison is given the powder absorption spectrum of 1 - 10 µm alumina particles either embedded in KBr or smeared onto a polyethylene plate. The arrow on Fig. 2 indicates the crossover between the two media. Alumina is trigonal so that the spectrum given in Fig. 2 is the superposition of two polarization directions. The Kramers-Kronig analysis identifies 5 bands of the 6 predicted by factor group analysis of the corundum structure (14).

The band wavenumbers may be compared with Barker's (14) measurements on oriented single crystals. The match is not perfect. Two intense bands that appear at 569 (perpendicular to the c-axis) and 583 $cm^{-1}$ (parallel) in the single crystal spectra are merged into a single intense band at 569 $cm^{-1}$ in the spectrum of the ceramic. Likewise, another intense pair of bands at 442 $cm^{-1}$ (perpendicular) and 400 $cm^{-1}$ (parallel) are merged into a single band at 428 cm-1. The lineshapes in the spectrum of the ceramic are very similar to those in the single crystal. In contrast, for this highly polar material there is only a slight resemblance between the powder spectrum and the single crystal phonon spectrum.

Fig. 3 shows the reflectance and dielectric loss spectra of a polished slab of limestone. The specimen is from the Mississippian Pahasapa formation collected from the southern Black Hills of South Dakota. It is a white, dense, coarsely crystalline calcite limestone with few impurities or minerals other than calcite. The high wavenumber modes in calcite are internal vibrations of the carbonate ion. The two bending bands at 710 and 872 $cm^{-1}$ are usually sharp even in powder spectra (15) and appear as weak, sharp modes in both single crystal and limestone spectra. The C-O stretching mode is the most intense band in the spectrum and appears at

1407 $cm^{-1}$ in the single crystal spectrum. In Fig. 3, this mode appears as a broad medium intensity band at 1481 $cm^{-1}$. Of the various ceramics examined in this study, the calcite stretching mode was the only band that was neither sharp nor in good agreement with single crystal values. This band is also greatly broadened in the powder spectrum. The low wavenumber bands are lattice modes and these also appear broadened in the powder spectrum. The lattice modes obtained from the polycrystalline specimen appear sharpened and in good wavenumber agreement with single crystal data (parallel: 303 and 92 $cm^{-1}$; perpendicular: 297, 223, and 102 $cm^{-1}$) but only three of the predicted 5 lattice bands are observed.

## IV. Analysis of Infrared Spectra: Quartz

To gain some insight into the relationship between deconvoluted IR reflectance spectra of ceramics and the IR spectra of oriented single crystals, a detailed study was made of quartz.

Because quartz is uniaxial there are two reflectance spectra; one measured with the electric vector of the incident radiation parallel to the crystallographic c-axis (Fig. 4) and the other with the electric vector perpendicular to the crystallographic axis (Fig. 5). What is immediately noticeable about the reflectance spectra is that the bands are very broad and have an unsymmetrical line shape. The dielectric loss function is shown for both crystallographic directions in Figs. 4 and 5. In the single crystal measurements the mathematical transforms that have been used here should produce correct line shapes and the maxima in the dielectric loss curve should correspond to the wavenumbers of the transverse optic modes. The line intensities and line halfwidths should also be an intrinsic property of the material. It should be noted that the infrared lines extracted from single crystal spectra are in fact very sharp, comparable in overall line shape to Raman spectra. Raman spectra measured on ceramic materials are known to produce correct line shapes (16).

For comparison, a powder infrared spectrum for quartz is shown in Fig. 6 plotted as absorbance against wavenumber rather than the more commonly used percent transmission. The contrast between the line shape and hence resolution in the powder spectrum and the dielectric loss spectrum is quite striking. Powder spectra typically contain very broad, poorly-resolved bands. The maxima on these bands do not match precisely with the vibrational modes determined from measurements on the single crystal. The powder spectrum is, of course a composite of the two single crystal spectra. Again the break indicated by the arrow in Fig. 6 indicates the shift from a KBr pellet spectrum measured in the higher wavenumber range and a polyethylene smear spectrum measured in the lower wavenumber range.

The spectra for three natural ceramics composed of silica are shown in Fig. 7. Chalcedony is a dense naturally-occuring form of silica with a fibrous habit and a grain size on the order of 0.1 μm. Chert is also very dense but has a grain size of 1 μm. Quartzite is a densely packed rock with sand-size quartz crystals in the range of 500 to 2000 μm. Though they share a common mineralogical makeup, these ceramics display distinct differences in their vibrational spectra, differences which set them apart both from one another and from single crystal quartz. Since one of the primary factors which differentiates these materials is grain size, it is natural to wonder whether considerations of grain size alone can be used to explain the observed spectra differences. In this section of the paper we have attempted to investigate the interplay between crystallite size and spectral properties by modifying single crystal quartz data in ways which depend on the grain size, comparing the resulting model spectra to the experimentally observed polycrystalline spectra.

The way in which light interacts with a single grain of material depends critically on the relationship between the size of the particle and the wavelength of the incident beam. The crystallites in chert and chalcedony fall into one category since they are much smaller than the wavelength of light used to probe the samples throughout the region of interest (8 to 25 μm). Grains sizes for both materials are less then 1 μm. These samples, then, are essentially isotropic and should behave as homogenous reflectors having an effective dielectric constant equal to that to a single quartz crystal averaged over all possible orientations.

$$\varepsilon_{eff} = \tfrac{1}{2}(2\varepsilon_{\perp} + \varepsilon_{\parallel})$$

Here $\varepsilon_{\perp}$ ( $\varepsilon_{\parallel}$ ) denotes the component of the dielectric function in the direction perpendicular (parallel) to the optic axis and was calculated via a Kramers-Kronig transformation of the single crystal reflectance data. Results are plotted in Fig. 8 ("Model 1").

The crystallites in quartzite, on the other hand are orders of magnitude greater than those in the fine-grained samples. Thus, each grain acts as independent reflector with randomly oriented optic axis. The averaging procedure required to construct the total reflection from a collection of such grains is not trivial because of their non-cubic symmetry, so instead we have made the approximation

$$R_{eff} = \tfrac{1}{2}(2R_{\perp} + R_{\parallel})$$

The resulting averaged spectrum was then transformed to yield values of the real and imaginary parts of the dielectric function, shown in Fig. 8 ("Model 2").

The model calculations can be compared with the experimental results in Fig. 9. Peak locations and, to a lesser degree, peak shapes correspond well. The combination of the single crystal 1066 and 1075 $cm^{-1}$ lines into a single feature in both the experimental and model spectra is the natural result of the presence of two peaks separated in wavenumber by an interval smaller than either of their linewidths and is not an artifact of the transformation procedure. The averaged position of this peak predicted by the model is observed experimentally to within 2 $cm^{-1}$.

The low-wavenumber region is where both the experimental spectra and the model spectra display the greatest amount of variability. For the fine-grained materials, peak locations are fairly well predicted by Model 1, but the observed bands have broadened and merged to an extent not seen in the model. The peaks in this region, however, correspond with bond bending vibrations, modes which are fairly easily distorted. Considering the large amount of surface area present within a fine-grained ceramic it is not surprising to find significant deviations from purely crystalline behavior in this region. The correspondence of the low-wavenumber quartzite spectrum with that of Model 2 is quite good; peak positions agree to within a few wavenumbers and lineshapes match up well.

The most striking features present in the quartzite spectrum are the regions in which $\varepsilon''$ dips below zero. In spectra of single crystals or isotropic materials the presence of an unphysical feature such as this is an indication that the reflectance data are inaccurate in some respect (the reflectance is non-specular, improperly normalized, etc). Since, however, this behavior is reproduced in the model but is not present in the single crystal spectra from which the model was constructed, we can conclude that the error lies not in the method of data collection but in the polycrystalline nature of the sample itself and in the subsequent data analysis.

The Kramers-Kronig transformation cannot accurately deconvolute spatially non-uniform reflectance data. This should not be a problem for fine-grained materials or even for coarse-grained materials in regions where reflectance is nearly independent of crystallographic orientation (as is the case for the high-wavenumber quartzite bands) since in both cases the reflectance is essentially isotropic. These expectations are borne out by both the model and the experimental spectra.

For a more quantitative comparison of model and experiment, the oscillator strengths, $\Delta\varepsilon$, of the major peaks have been calculated (Table II). The oscillator strength of a band is a useful quantity because it is a measure of the number of resonating oscillators per unit volume and is independent of linewidth. $\Delta\varepsilon$ is typically calculated by measuring the area, A, under the $\varepsilon''$ curve of band i and employing the relationship:

$$\Delta\varepsilon_i = (2/\pi)(A/\omega_i)$$

where $\omega_i$ is the peak wavenumber. This function depends on a number of assumptions, the most crucial of which is the assumption that the peak in question is well separated from its neighbors. Unfortunately, this condition is not met in the low wavenumber regions of the test case spectra where there is considerable overlap between pairs of bands. In these cases the value listed for $\Delta\varepsilon$ is a net oscillator contribution, calculated by estimating the area contribution for each band and adding together the resulting values of $\Delta\varepsilon_i$.

$$\Delta\varepsilon = (2/\pi)(A_1/\omega_1 + A_2/\omega_2)$$

The error introduced by this method can be evaluated by comparing the summed values to those obtained when all of the area is assigned to the largest peak, and is found to be no more than three percent.

A comparison of the oscillator strengths calculated for the model spectra with those of the polycrystalline spectra show excellent agreement. Values match to within a few hundredths except in the low wavenumber region of chert where somewhat larger errors were found.

## V. Conclusions

Infrared specular reflectance spectra measured from polished specimens of dense ceramic can be deconvoluted by Kramers-Kronig transformation to yield dielectric loss spectra with sharp, well-defined bands with proper line shapes. This approach to IR spectroscopy of polycrystalline polar materials eliminates the line shape distortion found in IR spectra of powders dispersed in dielectric media. However, certain caveats must be observed.

(i) Ceramics composed of cubic materials yield good spectra regardless of particle size (glasses can also be measured in this way). Some porosity can be tolerated with only a reduction in line strength.

(ii) For non-cubic materials, it is important that the particle size be small relative to the infrared wavelength of interest. Certain artifacts appear in the spectra of coarse-grained anisotropic materials, although these can be easily recognized as discussed under Model 2, above. Some line-broadening may be expected in the spectra of fine-grained materials if the grains have disordered surfaces.

(iii) When IR modes associated with different polarization directions fall within one band width of each other, they will appear as a single mode of intermediate wavenumber in the polycrystalline spectrum. This resolution limitation is a feature intrinsic to all reflection spectra and is not the result of experimental inadequacies or problems with the Kramers-Kronig transform. In such cases only single crystal spectra will resolve the individual modes.

## Footnotes

a. IBM Instruments model 98A, Danbury CT.

b. Spectra-Tech Inc., Stamford CT

c. Motorola Inc. Carlisle, PA

d. Coors Ceramics, Golden, CO

e. Irtran 4, Kodak Inc., Rochester, NY

## References

1. O.B. Toon and J.B. Pollack, "The Optical Constants of Several Atmospheric Aerosol Species: Ammonium Sulfate, Aluminum Oxide, and Sodium Chloride," J. Geophys. Res. **81** [33] 5733-5748 (1976).

2. J.R. Aronson, and P.F. Strong, "Optical Constants of Minerals and Rocks," Appl. Optics **14** [12] 2914-2920 (1975).

3. L. Genzel, A. Wittin, J. Kuhl, H.J. Mattausch, W. Bauhofer, and A. Simon, "Far-Infrared Spectroscopy of the High $T_c$ Superconductor $YBa_2Cu_3O_{7-}$ ," Solid State Comm. **63** [9] 843-846 (1987).

4. L. Genzel and T.P. Martin, "Infrared Absorption in Small Ionic Crystals," Phys. Status Solidi (b) **51**, 91-99 (1972).

5. G. Turrell, Infrared and Raman Spectra of Crystals. Academic Press, New York, NY, 1972.

6. T.K. Trout, J.M. Ballama, F.E. Brinckman, and R.A. Faltynek, "Fourier Transform Infrared Analysis of Ceramic Powders: Quantitative Determination of Alpha, Beta, and Amorphous Phases of Silicon Nitride," J. Mater. Res. **4** [2], 399-403 (1989).

7. F.E. Volz, "Infrared Specular Reflectance of Pressed Crystal Powders and Mixtures," Appl. Optics **22** [6], 1842-1855 (1983).

8. J.D. Axe and G.D. Petit, "Infrared Dielectric Dispersion and Lattice Dynamics of Uranium Dioxide and Thorium Dioxide," Phys. Rev., **151** [2], 676-680 (1966).

9. P.L. Provenzano, S.I. Boldish and W.B. White, "Vibrational Spectra of Ternary Sulfides with the $Th_3P_4$ Structure," Mat. Res. Bull. **12**, 939-946 (1977).

10. F. Gervais and J. Lecomte, "Infrared Reflectivity Analysis of Perovskite Ceramics $Sr(Sr_{1/3}Nb_{2/3})O_3$," Solid State Comm. **53** [8], 711-713 (1985).

11. M. Bliss and W.B. White, work to be published.

12. B.L. Walden and W.B. White, work to be published.

13. S.S. Mitra, "Infrared and Raman Spectra Due to Lattice Vibrations" Optical Properties of Solids, Chap. 14, Plenum Press, New York, 333-451 (1969)

14. A.S. Barker, Jr., "Infrared Lattice Vibrations and Dielectric Dispersion in Corundum," Phys. Rev. **132** [2] 1474-81 (1963).

15. W.B. White, "The Carbonate Minerals," The Infrared Spectra of Minerals, V.C. Farmer, Ed., Chap. 12, The Mineralogical Society of London, 227-284 (1974).

16. G. Burns, "Powder Raman Spectra: Application to Displacive Ferroelectrics," Mat Res. Bull., **6**, 923-930, (1971).

Table I. Sources of Specimens

| | |
|---|---|
| Silica | |
| Quartz Single Crystal | Hydrothermally Grown Synthetic (c) |
| Chalcedony | |
| Chert | |
| Quartzite | Tuscarora Formation, Reedsville, PA |
| Alumina | Sintered with 4 wt% Glass (d) |
| Zinc Selenide | Hot Pressed (e) |
| Calcite | Fine-Grained Limestone. Pahasapa Formation, Custer, SD |

## TABLE II.

Comparison of Observed Band Parameters with Single Crystal Data

| | $cm^{-1}$ | $\Delta\varepsilon$ | $cm^{-1}$ | $\Delta\varepsilon$ | $cm^{-1}$ | $\Delta\varepsilon$ | $cm^{-1}$ | $\Delta\varepsilon$ |
|---|---|---|---|---|---|---|---|---|
| Model 1 | 365/393 | 0.52 | 451/493 | 0.77 | 775/794 | 0.12 | 1068 | 0.61 |
| Chalcedony | 371/395 | 0.49 | 460 | 0.77 | 780/796 | 0.11 | 1070 | 0.61 |
| Chert | 373/394 | 0.40 | 461/528 | 0.73 | 783/798 | 0.10 | 1069 | 0.63 |
| Model 2 | | | | | 781/795 | 0.15 | 1067 | 0.63 |
| Quartzite | | | | | 781/799 | 0.13 | 1067 | 0.67 |

## Legends for Figures

Fig. 1 Reflectance spectra, dielectric loss spectrum and powder absorbance spectrum for hot-pressed ZnSe.

Fig. 2 Reflectance spectrum, dielectric loss spectrum and powder absorbance spectrum for tape-cast sintered alumina.

Fig. 3 Reflectance spectrum and dielectric loss spectrum for sawed and polished surface of limestone.

Fig. 4 Reflectance spectrum and dielectric loss spectrum for an oriented polished quartz crystal with infrared beam polarized with the electric vector parallel to the c-axis.

Fig. 5 Reflectance spectrum and dielectric loss spectrum for an oriented polished quartz crystal with infrared beam polarized with the electric vector perpendicular to the c-axis.

Fig. 6 Infrared absorbance spectrum of powdered quartz.

Fig. 7 Dielectric loss spectra of three forms of polycrystalline quartz.

Fig. 8 Calculated dielectric loss spectra for polycrystalline quartz. Model 1: average of the dielectric loss spectra for the two crystal orientations. Model 2: average of the reflectance spectra for the two crystal orientations followed by Kramers-Kronig analysis of the composite reflectance spectrum.

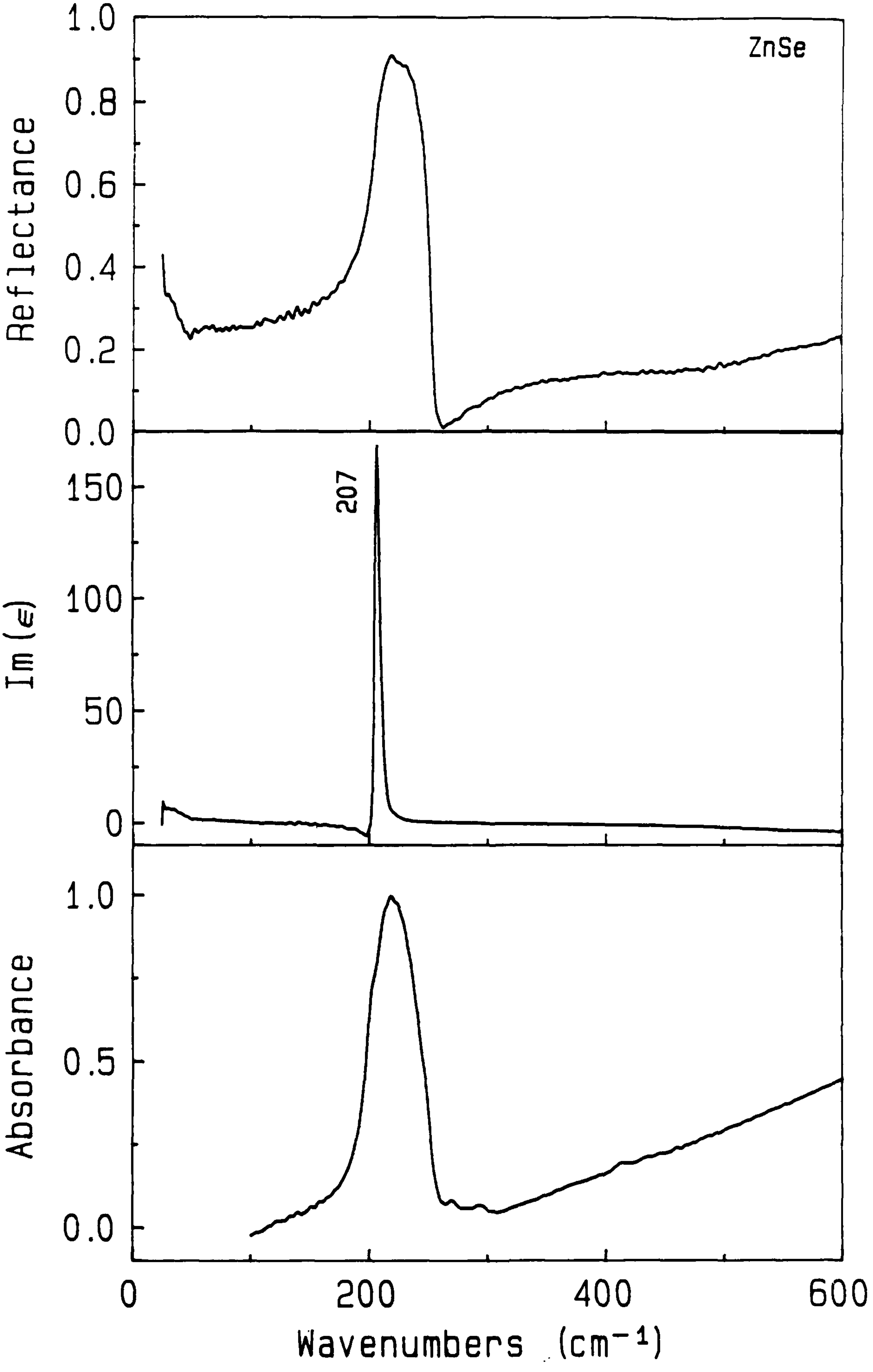
ZnSe
Reflectance
1.0
0.8
0.6
0.4
0.2
0.0
Im(ε)
150
100
50
0
207
Absorbance
1.0
0.5
0.0
0
200
400
600
Wavenumbers (cm⁻¹)

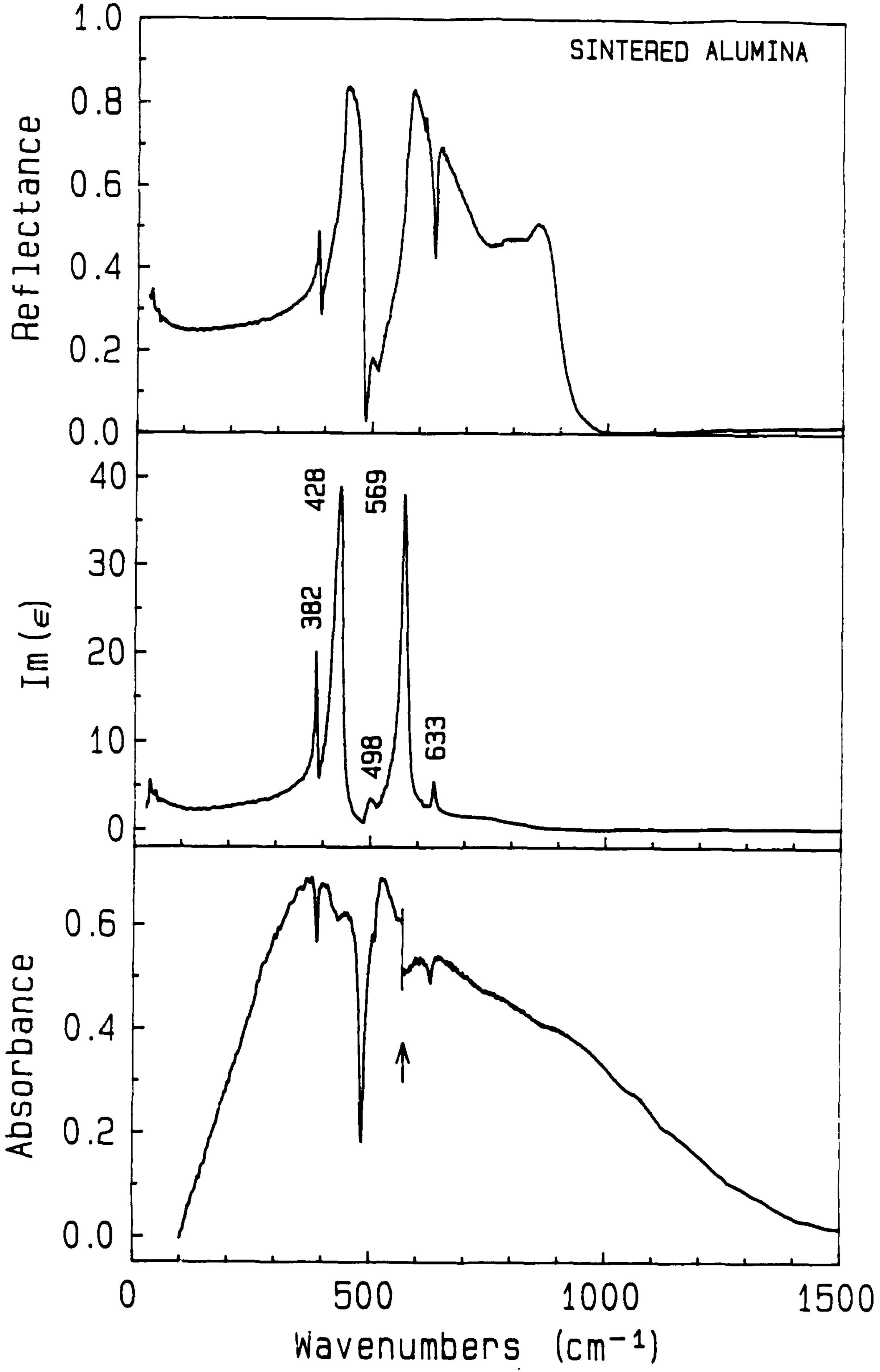

SINTERED ALUMINA
Reflectance
1.0
0.8
0.6
0.4
0.2
0.0
Im (ε)
40
30
20
10
0
428
569
382
498
633
Absorbance
0.6
0.4
0.2
0.0
0
500
1000
1500
Wavenumbers (cm⁻¹)

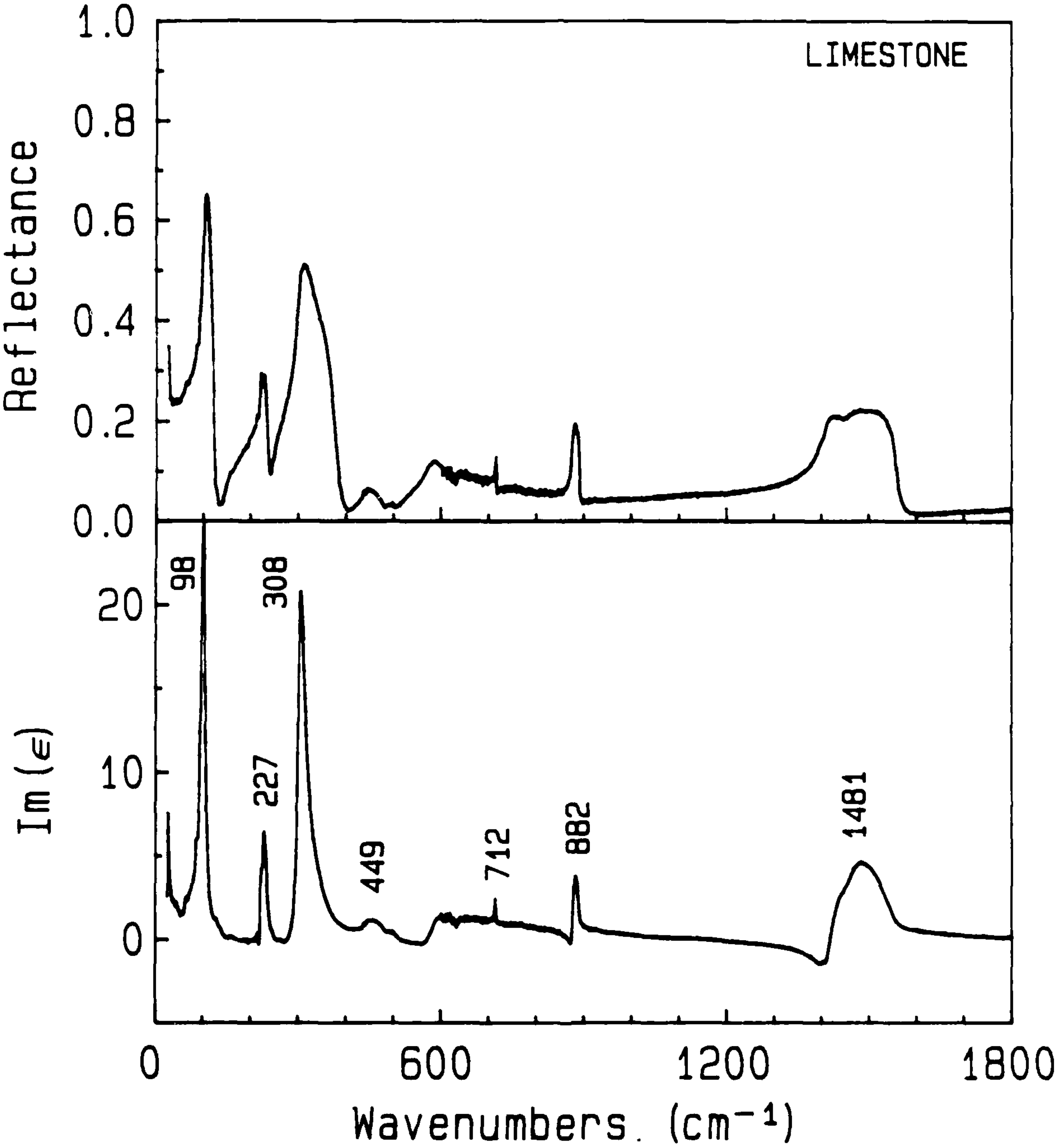

1.0
0.8
0.6
0.4
0.2
0.0
Reflectance
LIMESTONE
20
10
0
Im (ε)
98
308
227
449
712
882
1481
0
600
1200
1800
Wavenumbers (cm⁻¹)

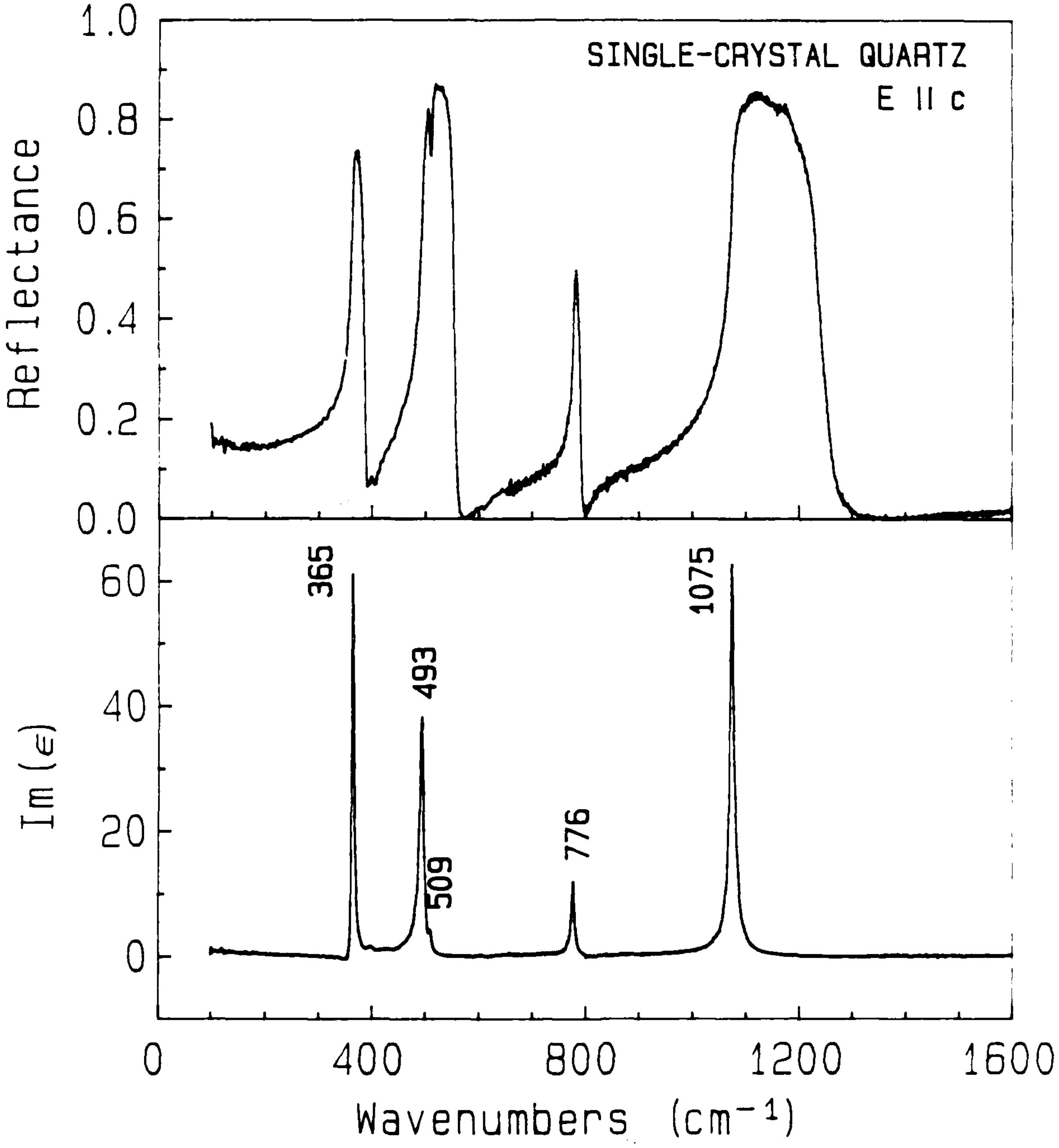
SINGLE-CRYSTAL QUARTZ
E ‖ c
Reflectance
1.0
0.8
0.6
0.4
0.2
0.0
Im(ε)
60
40
20
0
365
493
509
776
1075
0
400
800
1200
1600
Wavenumbers (cm⁻¹)

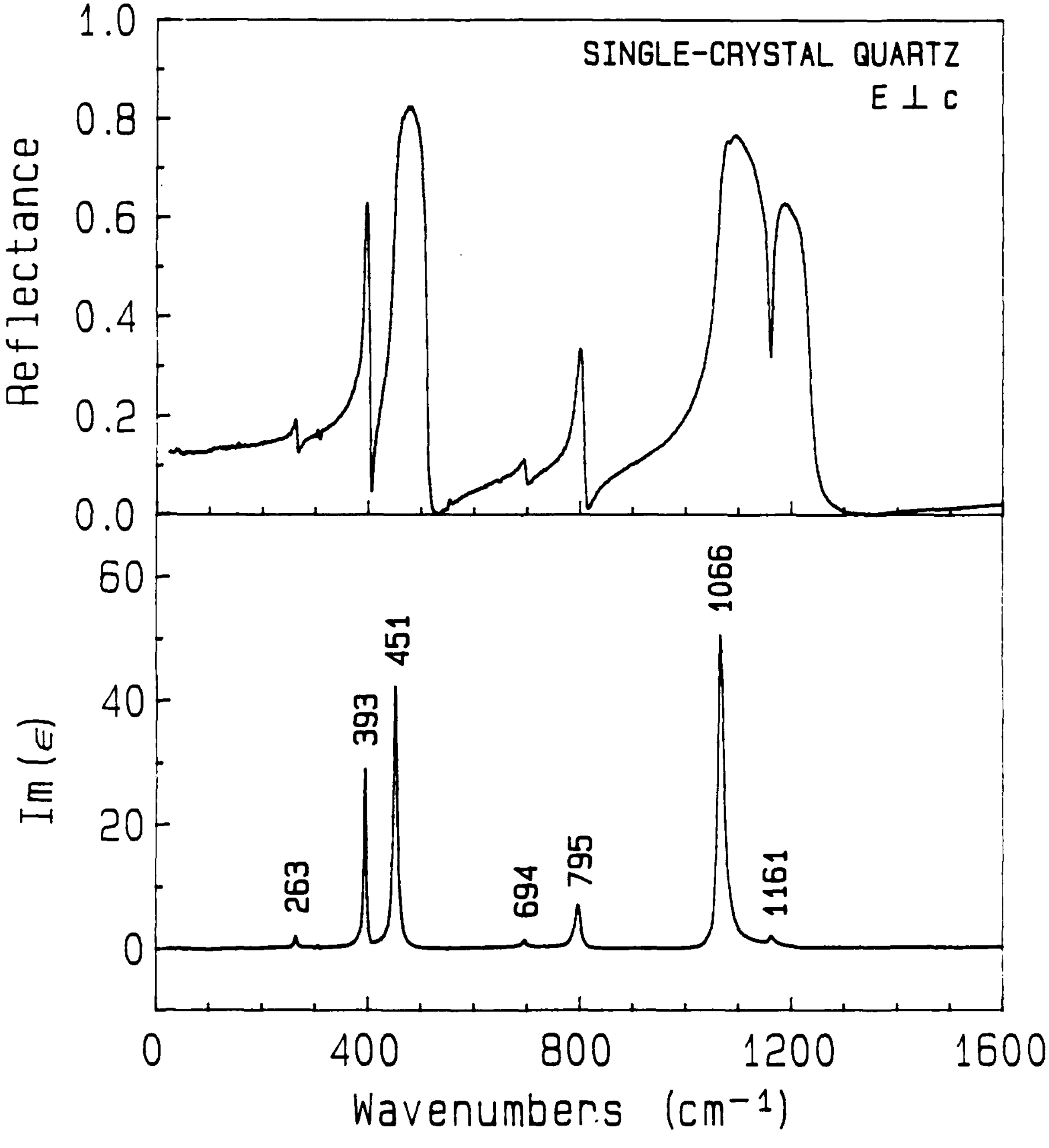
SINGLE-CRYSTAL QUARTZ
E ⊥ c
Reflectance
1.0
0.8
0.6
0.4
0.2
0.0
Im (ε)
60
40
20
0
263
393
451
694
795
1066
1161
0
400
800
1200
1600
Wavenumbers (cm⁻¹)

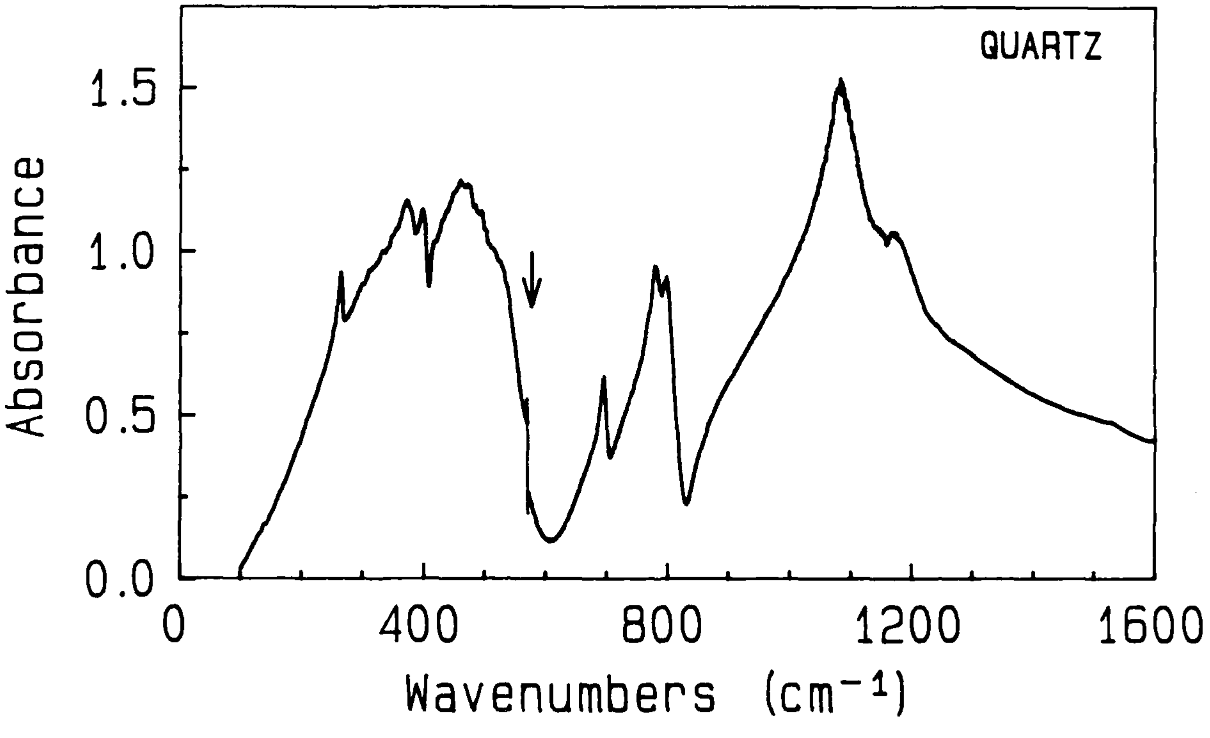
QUARTZ
Absorbance
0.0
0.5
1.0
1.5
0
400
800
1200
1600
Wavenumbers (cm⁻¹)

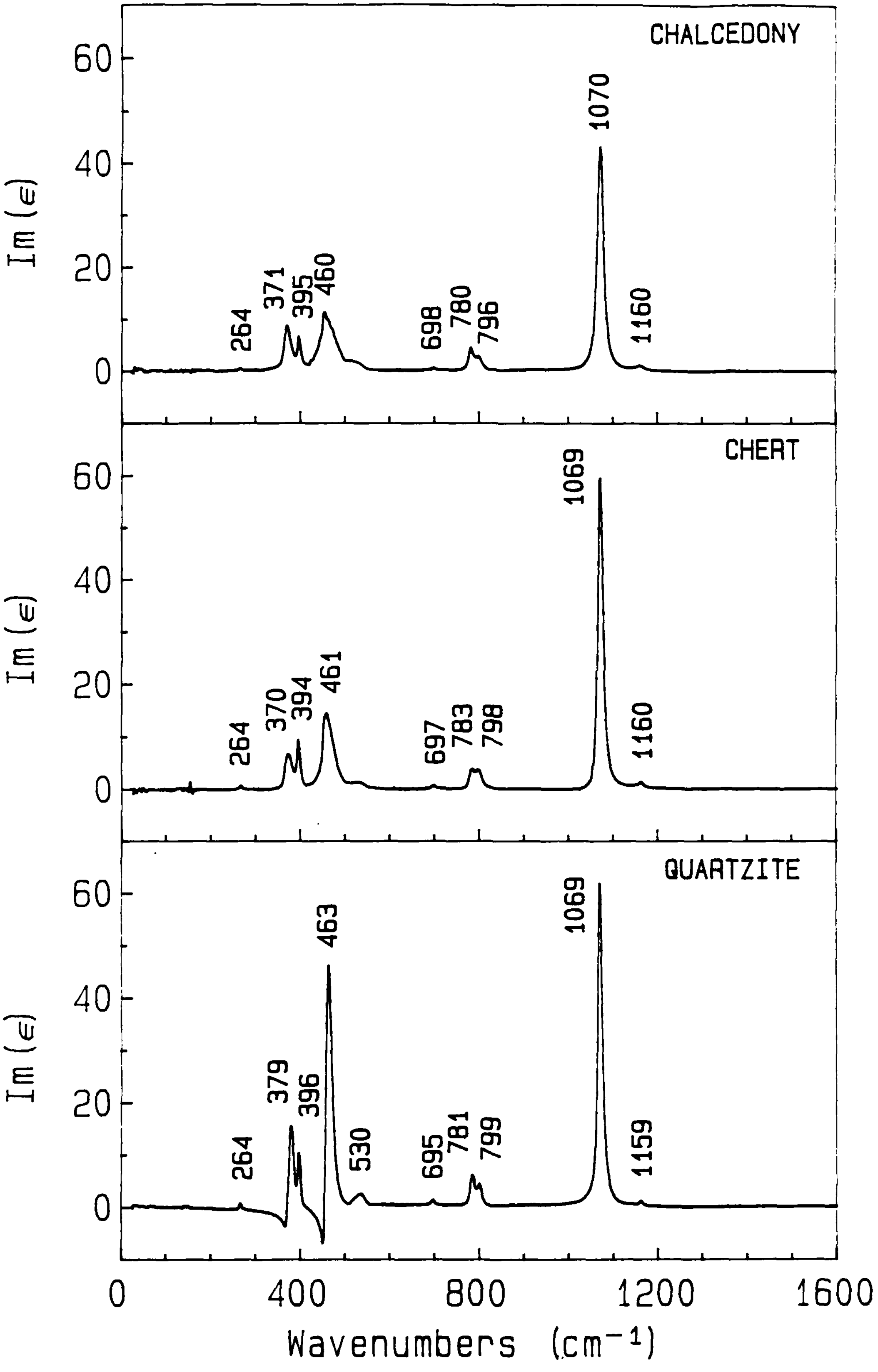
CHALCEDONY
CHERT
QUARTZITE
Im (ε)
60
40
20
0
264
371
395
460
698
780
796
1070
1160
264
370
394
461
697
783
798
1069
1160
264
379
396
463
530
695
781
799
1069
1159
0
400
800
1200
1600
Wavenumbers (cm⁻¹)

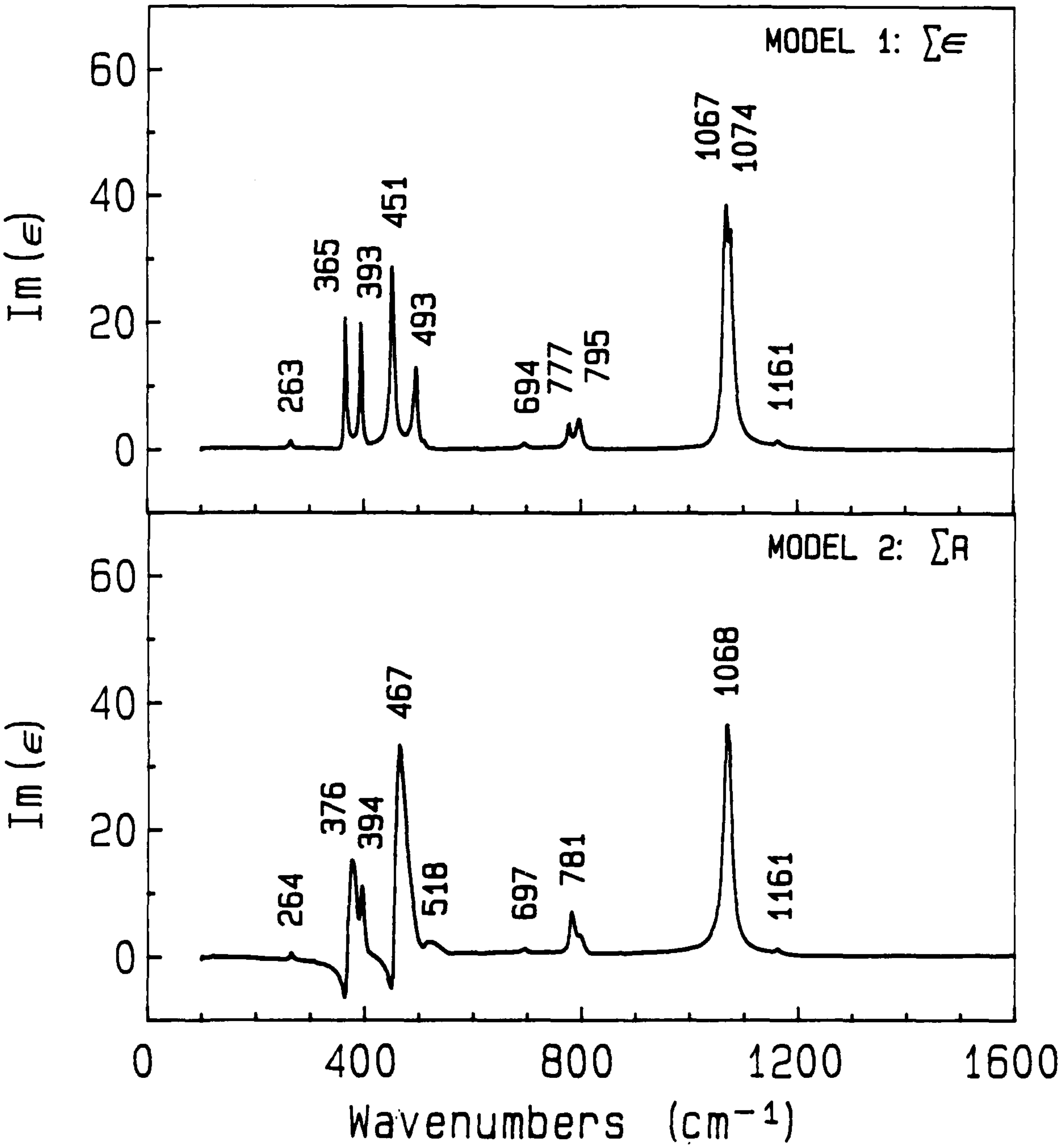
MODEL 1: ∑ε
MODEL 2: ∑A
Im (ε)
Im (ε)
60
40
20
0
60
40
20
0
263
365
393
451
493
694
777
795
1067
1074
1161
264
376
394
467
518
697
781
1068
1161
0
400
800
1200
1600
Wavenumbers (cm⁻¹)